The Impact of *Seasat-A* Scatterometer Data on High-Resolution Analyses and Forecasts: The Development of the *QE II* Storm

A. C. M. STOFFELEN AND G. J. CATS

Royal Netherlands Meterological Institute (KNMI), DE BILT, The Netherlands

(Manuscript received 5 May 1990, in final form 22 April 1991)

ABSTRACT

In this paper the impact of Seasat scatterometer winds in numerical weather prediction (NWP) is discussed with the help of the results of some cases studied.

The development of the *Queen Elizabeth II* (*QE II*) storm from 1200 UTC 9 September to 0000 UTC 11 September 1978 is analyzed and forecast with a high-resolution (60-km) limited-area model (LAM). Parallel assimilation and forecasts are performed; in the SCAT run, Seasat scatterometer winds were used, but from the parallel NOSCAT run these winds were omitted.

The NOSCAT analyses catch the development of the *QE II* storm better than any other operational numerical weather prediction model did, to our knowledge. When Seasat surface winds were included, the wind and sea level pressure were analyzed even better. Also, the forecasts improved substantially.

We expect that the impact of these winds in NWP models can be enhanced not only by further research on and development of assimilation methods, but also by an improved representation of the upper-air structure.

1. Introduction

The improvement of forecast skill close to and over the oceans is most probably hampered by the lack of adequate observational data. In these regions surface data are limited to the conventional observations from buoys and ships; a few upper-air observations are available from islands, automated soundings on trade ships, and ocean weather ships. The observational, temporal, and spatial density may be insufficient to determine the initial state for high-resolution limited-area models (LAMs). Remote sensing (RS) satellite observations might be able to fill this data gap.

This study is concerned with the use of sea surface winds from the *Seasat-A* Scatterometer System (SASS), which flew from July to October 1978. The instrument emitted a centimeter-wavelength radar beam and measured the backscattered power from capillary ocean waves; these waves are correlated with wind speed and direction. Indirectly, the normalized backscattered power is related to the wind vector (Pierson 1983).

To measure the impact of SASS data on numerical weather prediction (NWP), parallel assimilation studies were carried out. In these studies experiments that include scatterometer winds (SCAT) are compared with experiments that exclude these winds (NOSCAT). In global impact studies using coarse-resolution (grid distances > 140 km) NWP models, substantial effects were observed in the Southern Hemisphere and tropics when SASS data were included. On the other hand in the Northern Hemisphere the impact was small (Anderson et al. 1987; Yu and McPherson 1984; Duffy et al. 1984; and Baker et al. 1984).

The distance between neighboring SASS observations is 100 km within the swath; these scales cannot be resolved by the analysis systems in global models (resolution > 200 km). Only a high-resolution LAM analysis might be able to resolve these scales. Also, geostrophic-adjustment theory shows that wind observations become more important on smaller scales, compared to temperature and pressure observations. These arguments suggest that SASS data might have a positive impact in the Northern Hemisphere on higher-resolution analyses.

Meteorologists hope that scatterometer observations will be of help in detecting fast-developing systems. For example, the rapid development of the *Queen Elizabeth II* (*QE II*) storm from 1200 UTC 9 September to 0000 UTC 11 September 1978 was not adequately forecast by operational meteorological centers. The storm occurred close to the coast of Newfoundland. It began as a shallow baroclinic disturbance close to Cape Cod. The fishing trailer *Captain Cosmo* was lost close to Georges Bank after it had reported 5–6-m waves. The thermodynamic structure and development of the storm are well studied by Gyakum (1983a,b) and Anthes et al. (1983). According to an estimate of Gyakum (1983a), which we will use as a reference, the storm deepened 60 mb during its move-

Corresponding author address: Mr. Ad Stoffelen, European Centre for Medium Range Weather Forecasts (EC MWF), Shinfield Park, Reading, Berkshire, United Kingdom.

ment out over the ocean within 24 h to a minimum mean sea level pressure p(MSL) = 945 mb at 1200 UTC 10 September. At this time the barograph of the *Euroliner* measured a minimum pressure of p(MSL) = 956 mb in the vicinity of the center of the storm. At 0800 UTC 11 September the liner *QE II* turned south to avoid further damage from the 12-m waves at wind speeds of 30 m s^{-1} and over. The operational NMC model forecast wind speeds of 15 m s^{-1} and waves of only 3-m height in this area.

In 1983 Aune and Warner reported on a case study of the *QE II* storm with a global model (4° × 5°) and found only little impact of the SASS winds in agreement with the results of Anderson et al. (1987) and Yu and McPherson (1984), mentioned before.

Using a LAM, Duffy and Atlas (1986) tried to improve on the scatterometer impact. The model had 11 layers and a 100 × 100 km^2 horizontal resolution. In the modified Cressman analysis scheme the SASS observations could not alter the mass field, but observational wind increments at the ocean surface with regard to the analysis input field were allowed to change higher-level winds according to a vertical correlation function. Duffy and Atlas showed that the maximum surface wind speed in the 36-h forecast is increased from 21 to 37 m s^{-1} and the minimum p(MSL) decreased from 1000 to 988 mb. In spite of these improvements, the positional error was still rather large. Anderson et al. (1987) were able to produce a better forecast with the global ECMWF model, both with and without SASS data. However, they again found no impact of the SASS winds.[1]

Brown and Levy (1986) assimilated the scatterometer information in a two-layer atmospheric boundary-layer (ABL) model with a horizontal resolution of 50–100 km. They succeeded in improving the surface analysis of Anderson et al., especially at 1200 UTC 9 September; i.e., the development phase of the storm. Their numerical analysis of the sea surface pressure was very close to the synoptic estimate of Gyakum. This gives confidence in the ability to analyze and forecast the *QE II* storm in an adequate manner at high resolution and in the possibility to have some positive impact from the SASS data.

The organization of this paper is as follows. In the next section the data assimilation and forecasting system is explained. In particular we will discuss the features of interest to the assimilation of satellite surface observations. Section 3 describes observations used in our experiments. Sections 4 and 5 show the results obtained from the parallel assimilation and forecasting experiments, respectively. In section 6 we evaluate the impact of scatterometer data on the analysis of another storm—the *Ark Royal* storm—that occurred over the North Atlantic during the period Seasat was in orbit. We include this section because the differences between the analyses of the two storms give an indication of the situation in which maximum impact of the scatterometer winds may be expected. Our conclusions are presented in the last section.

2. The data assimilation and forecasting system

The data assimilation scheme used for the LAM at the Royal Netherlands Meteorological Institute (KNMI) is a 3-h intermittent cycle of analysis, initialization, and guess field (i.e., 3-h forecast), as shown in Fig. 1.

In the analysis the guess field is used as a background. For each observation the difference between the observed value and the guess-field value, interpolated to the observational position, is calculated. This increment, if judged to be correct by the observations quality control procedures, is interpolated to neighboring grid points by three-dimensional multivariate optimum interpolation (OI) of mass and horizontal wind (Cats 1984). The spatial correlation of the interpolated increments is a product of empirical horizontal and vertical correlation functions. The interpolation is done on 11 vertical standard pressure levels. Some further important properties of the OI scheme within the context of the SASS study are summarized below.

- Guess-field winds are extrapolated from the lowest model level (70 m) to observational height (10 m for SASS) by a simple logarithmic profile using the surface roughness z_0 (calculated by Charnock's formula).
- The vertical correlation of wind increments at the 1000-mb level with those at higher levels is given in Fig. 2.
- The horizontal correlation of the increments is calculated by Gaussian functions with a typical decay length of 300 km.
- The analyzed surface (e.g., SASS) increments are directly assigned to the 1000-mb level.

After interpolation to the forecast-model levels, the increments are added to the guess field to give the final analysis.

To the analysis fields we apply a bounded derivative initialization scheme to filter spurious gravity waves. The algorithm is equivalent to nonlinear normal-mode initialization schemes (Bijlsma and Hafkenscheid 1986).

The limited-area forecast model is a gridpoint model operating on 11 σ levels. The model time step is 3 min. The model is a descendant of the global ECMWF gridpoint model (Louis 1979). Radiative and convective processes and the horizontal diffusion have been adapted to the higher resolution.

The horizontal grid used to make the analyses and forecasts of the *QE II* storm is shown in Fig. 3. The

[1] Recent experiments with the 2° lat × 2.5° long version of the GLA global forecast model also show a substantial improvement over the Duffy and Atlas results and indicate a modest beneficial impact of SASS data (R. Atlas 1990, personal communication).

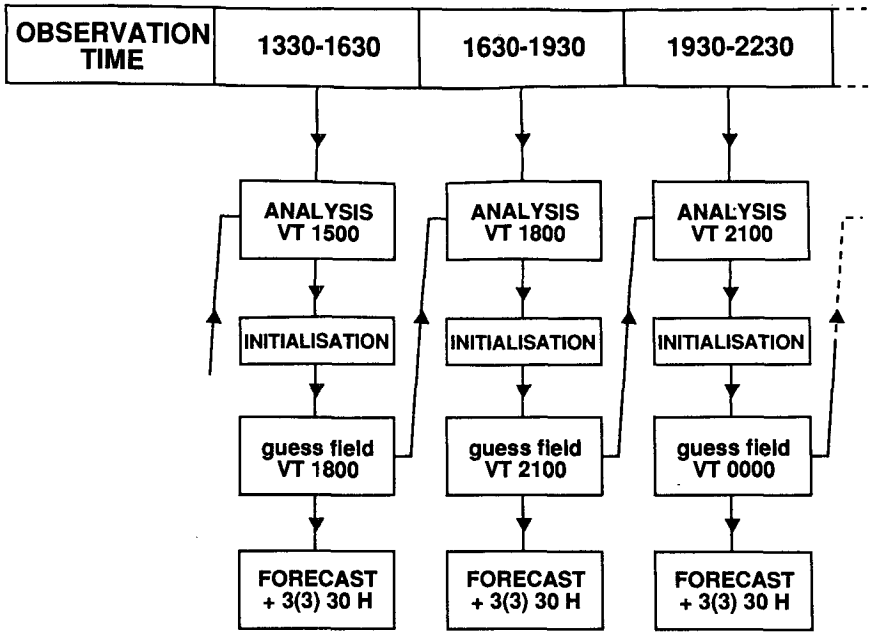

FIG. 1. Three-hourly intermittent assimilation scheme as used for LAM.

grid consists of 66 longitudinal and 61 latitudinal points in a transformed latitude–longitude projection with shifted pole (the North Pole is at 30°N, 180°). Grid distances are 0.55° (approximately 61 km).

To define our lateral boundaries we used fields interpolated from global analyses at T106 spectral resolution [the analyses are from the SASS impact study of Anderson et al. (1987) and include scatterometer information]. These fields are geopotential and horizontal wind components on 30, 100, 150, 200, 250, 300, 400, 500, 700, 850, and 1000 mb and humidity on 500, 700, 850, and 1000 mb.

Surface boundary conditions (e.g., sea surface temperature) are derived from monthly climatology.

The orography is obtained from mean surface heights on 1/6° × 1/6° squares, by averaging the heights of the squares that are centered in the area closest to the grid point under consideration.

3. Observations

Reports from surface land (SYNOP) and sea platforms (SHIP), radiosondes (TEMP), pilots (PILOT), and drifting buoys (DRIBU) were used in both SCAT and NOSCAT runs. Cloud-track–derived satellite winds (SATOB), aircraft reports (AIREP), and satellite temperature soundings (SATEM) are not used. The number of observations available and the estimated 1000-mb wind errors due to measurement and sampling errors are shown in Table 1. From the table we see a wealth of SASS data is available.

We estimated the SASS errors from collocation studies with SHIP observations (Anderson et al. 1987) and from internal consistency checks (Woiceshyn et al. 1986; Roquet and Ratier 1988). These internal checks pointed out that the SASS wind errors are not only dependent on wind speed, but also on the polar-

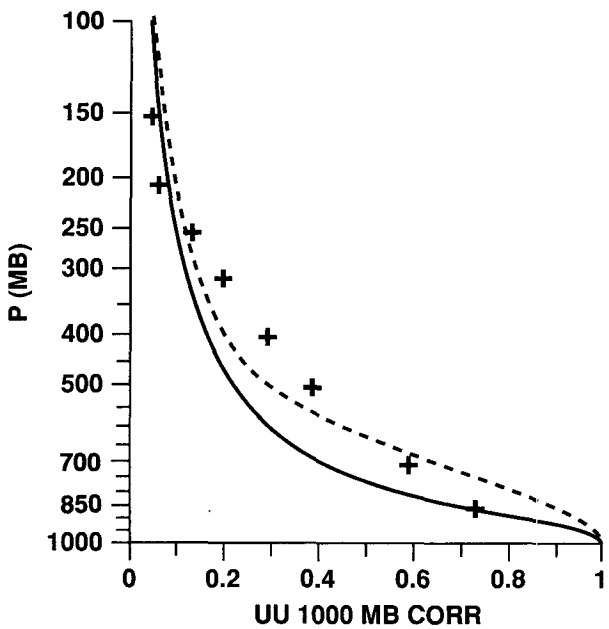

FIG. 2. The modeled correlation of a 1000-mb-level wind component increment, with the increments of the same wind component at other pressure levels. The solid and dashed line and the +'s are, respectively, used by Anderson et al. (1987) and Duffy et al. (1986) and us.

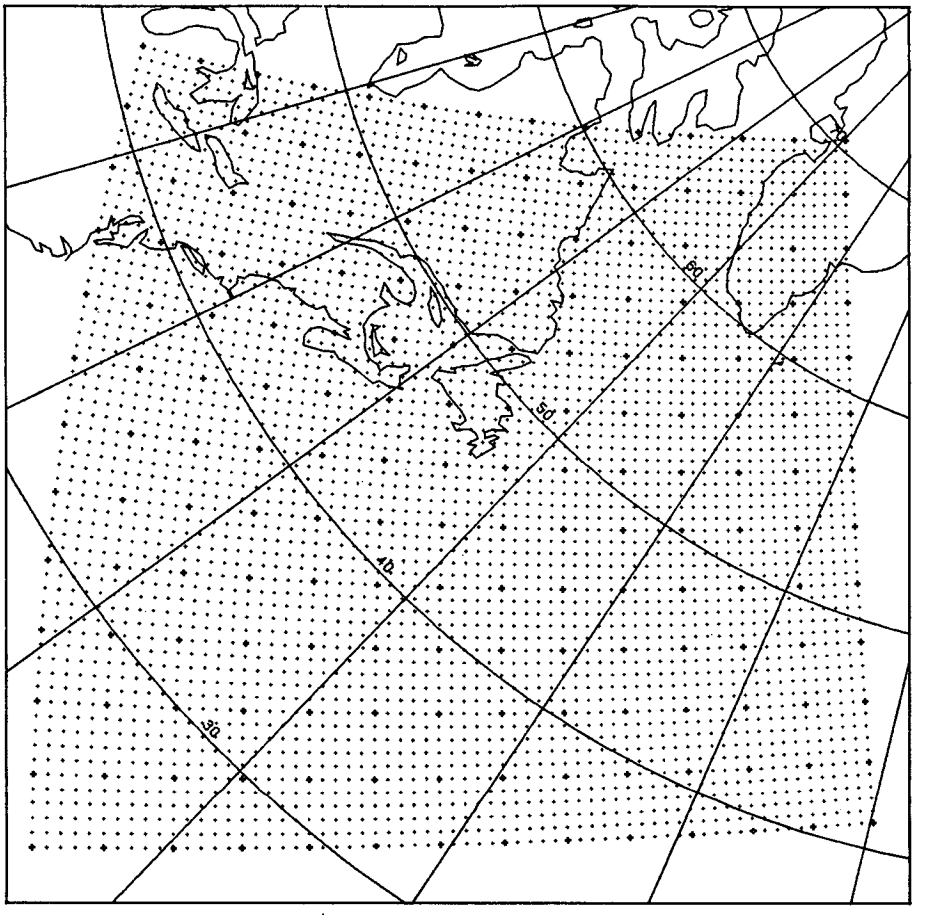

FIG. 3. Horizontal LAM grid used to forecast the *QE II* storm.

ization and incidence angle of the radar beam during measurement, and the wind direction relative to the propagation direction of the satellite. We did not include these dependencies in the estimate for a SASS wind error.

Moreover we assimilated the SASS winds just like SHIP or BUOY winds, neglecting some essential differences between those:

- Due to the empirical relationship used for the retrieval of winds from the backscatter measurements, and errors in the wind direction ambiguity removal procedure (dealiasing), horizontal correlations are introduced between the observation errors of neighboring SASS reports. SHIP observation errors are mutually uncorrelated.
- A SASS measurement represents the wind averaged over approximately one LAM grid cell. A SHIP observation is a spot measurement.
- SASS winds are asynoptic and most SHIP observations are synoptic.
- SASS observations lie within an observationally dense measurement swath, and SHIP observations occur at apparently random spots with considerably less density.

Furthermore, the assimilation systems of today have been developed with and for these conventional observations and are not yet adapted to satellite-derived measurements.

The SASS dataset we used was binned into squares of 100×100 km^2, containing 3–5 backscattered power measurements. The dealiasing procedure was carried out manually by two independent teams of meteorologists (see Wurtele et al. 1982; or Anderson et al. 1987).

TABLE 1. Number and surface error charcteristics of the observations used in the assimilation (f is wind speed in meters per second).

Observation type	Total number	Number per cycle	Estimated error for surface wind component (m s^{-1})
SYNOP	1642	37	3.0
SHIP	1871	43	3.0
TEMP	246	6	2.0
SASS	3784	86	$3.5 + (f - 10)1.9f \times 10^{-3}$

Figure 4 depicts the SASS observations measured at 1200 UTC 9 September and 1200 UTC 10 September of September 1978, together with the NOSCAT sea level pressure analysis. We see that, especially at 1200 UTC 10 September (Fig. 4b) cross-isobaric winds are present far east of the low pressure system; these are probably due to errors in the dealiasing procedure. We also note a positional error in our NOSCAT analysis.

According to Gyakum, at this time the maximum wind speed in the vicinity of the storm should be 37 m s^{-1}; i.e., as large as 70 kt. SASS observations show only wind speeds up to 60 kt, which visualizes their insensitivity for the measurement of high wind speeds (Anderson et al. 1987).

Because of its high resolution the scatterometer system is able to measure small-scale structures, fronts, and the precise position of a storm. The *QE II* storm in its development phase at 1200 UTC 9 September (Fig. 4a) is covered fairly well by the scatterometer observations.

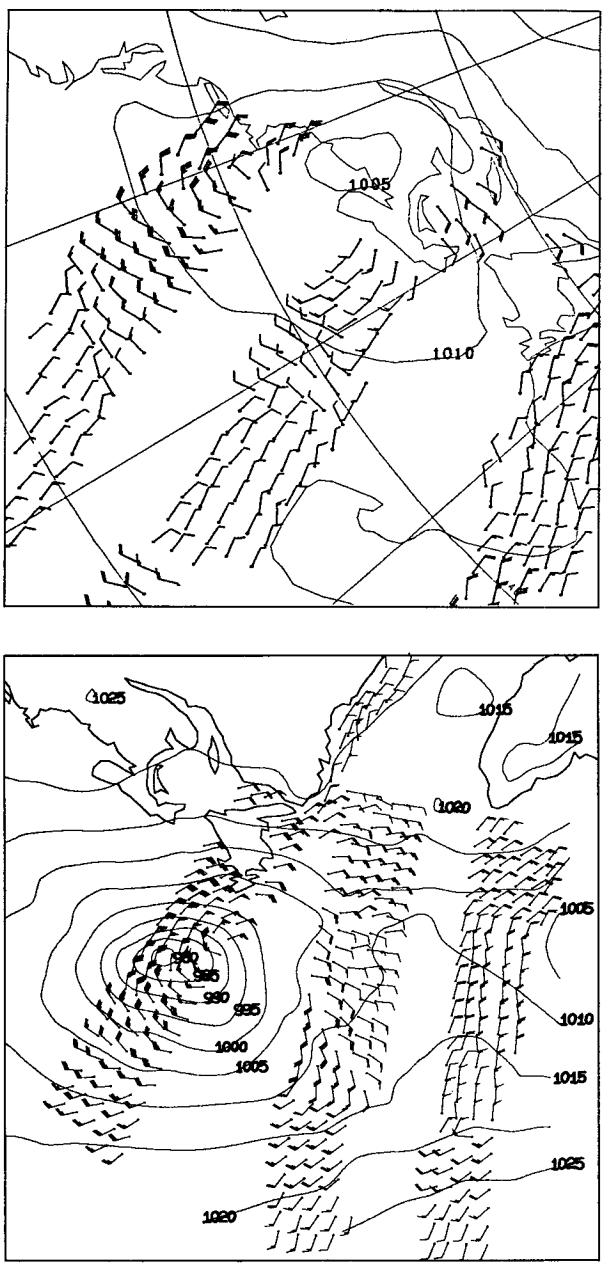

FIG. 4. SASS fleches plotted on a map of NOSCAT-analyzed mean sea level pressure (mb) at 1200 UTC 9 September (a) and 1200 UTC 10 September (b). The observations shown are used at this time.

4. Assimilation results

We did a SCAT run in which all observational data were used and a NOSCAT run in which SASS data were excluded. We ran 44 3-h cycles in these two parallel assimilation sequences, starting at 0600 UTC 6 September.

In Fig. 5a we see the SCAT-minus-NOSCAT analysis difference for surface wind at 1200 UTC 9 September. At this time many SASS winds were available. We observe small-scale coherent structures introduced by these observations. At other analysis times when many scatterometer winds are also present, similar structures in the SCAT-minus-NOSCAT differences are observed. Of course, an obvious explanation for the coherence is in the fact that the analysis scheme uses Gaussian correlation functions with a horizontal decay length of 300 km, in combination with the assumption of geostrophic and nondivergent analysis increments.

The analyzed track of the *QE II* storm, shown in Fig. 6, appeared not to be significantly different for SCAT and NOSCAT analyses (within one or two grid distances) and compares better with the German manual analyses given in the European Meteorological Bulletin (1978) than the analyses described in Anderson et al. (1987). To our knowledge, Anderson's analyses describe the *QE II* storm track better than any other operational model. This indicates that among those above, our analyzed SCAT and NOSCAT storm tracks are the most accurate.

In Fig. 7 the time evolution of the minimum surface pressure and the maximum wind speed in the vicinity of the storm are shown as obtained by a number of analysis schemes. We can see that only the LAM correctly diagnoses the rapid deepening between 0000 and 1200 UTC 10 September, as estimated by Gyakum (1983a). Also, note that the scatterometer data improve the analyses substantially; most remarkable is the explosive increase of maximum wind speed as analyzed by the SCAT analyses (and not by the NOSCAT analyses).

To evaluate the transport of SASS information in the model, it is interesting to trace how the differences survive initialization and model integration. Initialization effects on surface pressure and 500-mb heights were occasionally as large as 4 mb and 40 m, respectively. SCAT-minus-NOSCAT height differences are smoothed at 1000 and 500 mb, but the main features

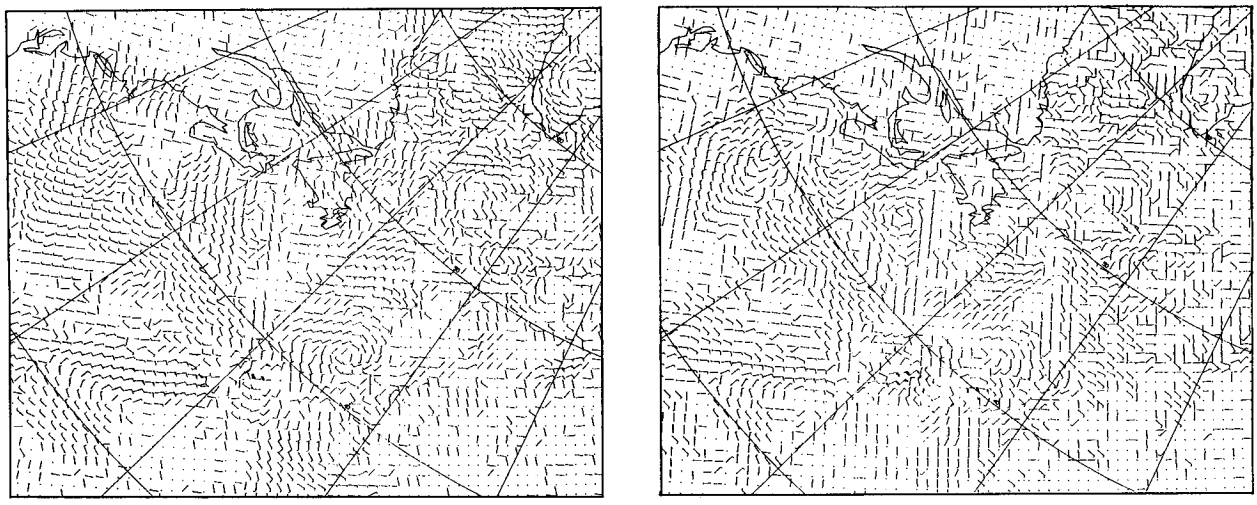

FIG. 5. SCAT-minus-NOSCAT 10-m-level wind vector differences: (a) analysis differences for 1200 UTC 9 September and (b) guess-field differences for 1500 UTC 9 September of September 1978 (3 h later).

introduced by the SASS data remain. In Fig. 5b the guess-field differences, verifying 3 h later than the field of Fig. 5a, are shown. In general, the scale of the SASS-introduced guess-field structures is larger than that of the analysis in both the horizontal and vertical directions, but on average the amplitude of the differences is smaller both at 1000 and 500 mb. Consequently, information from SASS data survives during initialization and 3-h model integration.

5. Forecast results on the *QE II* storm

We made two sets of two parallel forecasts over the period of rapid development of the storm; one from 1200 UTC 9 September when a wealth of SASS data were available and one from 0000 UTC 10 September, when in the preceding four assimilation cycles no such data had been available in the area of interest. The forecast tracks of the storm agree very well with the analyzed tracks as shown in Fig. 6. In Fig. 8 the predicted minimum mean sea level pressure is shown for all four runs. We note that the development of the storm is also described excellently in comparison to other forecast models, and that the SCAT forecast from 1200 UTC 9 September performs much better than the NOSCAT forecast.

During the first 12 h of model integration (until 0000 UTC 10 September), the differences between SCAT and NOSCAT are subtle, which also becomes apparent from Fig. 8. With respect to the vertical, the forecast SCAT-minus-NOSCAT differences were generally largest at the surface; there was no vertical tilt in the structures of the differences.

The SCAT forecast from 0000 UTC 10 September is still slightly better than the NOSCAT forecast. So although the differences are small, some useful scatterometer information from 1200 UTC 9 September is still present after four subsequent assimilation cycles in the analysis of 0000 UTC 10 September.

In this section we mainly described the forecast results on the *QE II* storm. A further discussion in relation to the results on the *Ark Royal* storm will be given in the next section.

6. The *Ark Royal* storm

Between 0600 and 2100 UTC 16 September 1978 a trough located northwest of Scotland developed into a major storm, with a central pressure of 960 mb. This storm is often named after a U.S. Navy vessel that remained in its vicinity, the *Ark Royal*. The impact of scatterometer data on the treatment of this storm by the ECMWF model has been described by Anderson et al. (1987), and a detailed description of the results with the LAM is found in Stoffelen et al. (1990). Here we give only those results that we believe to be relevant

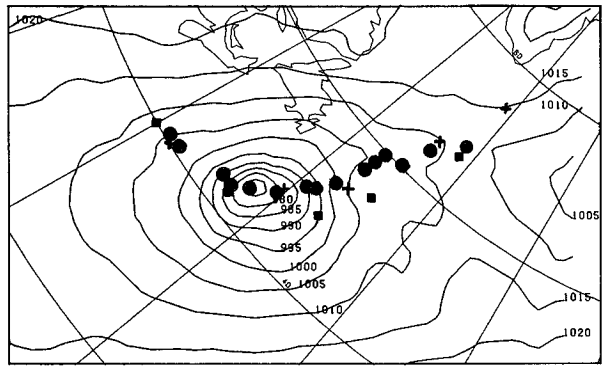

FIG. 6. The track of the *QE II* storm as analyzed by the German manual analysis + by Anderson et al. (1987) using SASS ■, and with LAM in experiment SCAT ●. The ■ and + are for 0000 UTC 10 September until 0000 UTC 12 September in 12-h steps. The ● is for 0300 UTC 10 September until 1800 UTC 11 September in 3-h steps. The background field is the SCAT analysis from 1200 UTC 10 September.

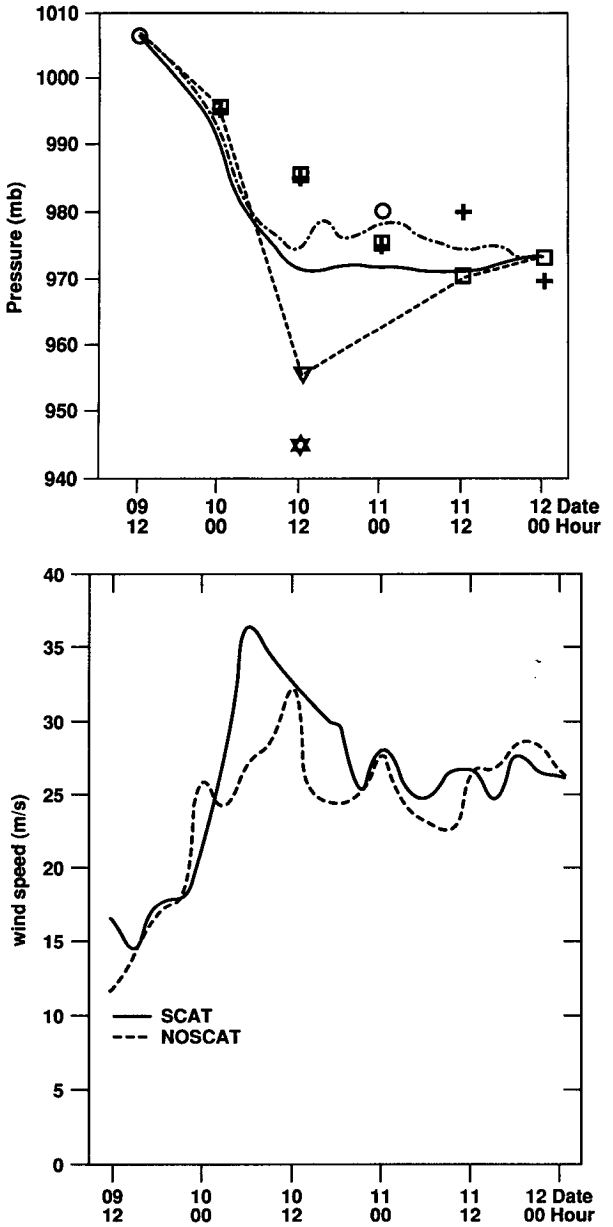

FIG. 7. Time evolution as produced by a number of analyses of (a) minimum surface pressure: + German analysis, □ Anderson et al. (1987), ▽ Anthes (1983) 100-km estimate, ☆ Anthes (1983) spot estimate, – – truth (subjective, Gyakum 1983a) ·-·- NOSCAT analyses, and —— SCAT analyses; (b) maximum wind speed: – – NOSCAT analyses, and —— SCAT analyses.

for the generalization of the scatterometer impact, as seen in the *QE II* case, to other situations.

The SCAT guess field and scatterometer data near the initial trough are shown in Fig. 9. Forecasts from both the NOSCAT and the SCAT analyses failed to predict the rapid development of this trough. The SCAT analysis of 2100 UTC 16 September (Fig. 10) has a central pressure of 960 mb, but the +12-h forecasts show only 973 mb (NOSCAT) and 970 mb (SCAT).

Examination of Fig. 9 led us to suspect that the scatterometer wind vectors have not been dealiased properly for wind direction. Because dealiasing has been done subjectively with reference to, indeed, all available, but still sparse meteorological information, a wrong direction may have been chosen here.

To corroborate this, the SCAT analysis was redone, but with the suspected wind directions of the scatterometer data replaced by the alias closest to the guess-field wind direction. This led to a sharper trough in the analysis, but unfortunately the effect on the subsequent forecasts was relatively small, as shown in Fig. 10.

We have tried to identify a cause for the differences in the *QE II* and the *Ark Royal* storm runs, both in the quality of the NOSCAT forecasts and in the improvements obtained by the additional use of the scatterometer data. The most plausible explanation we could think of is the following. The rapid development of both storms shows that the flow must have been (baroclinically) unstable. The structure of the upper-air flow was relatively well known in the *QE II* case, because of the good radiosonde coverage upstream over North America. Therefore, the LAM forecast model was well able to predict the rapid growth of an initial disturbance. The presence of the disturbance was analyzed in the NOSCAT run, and even better, both for position and intensity, in the SCAT analysis.

In the *Ark Royal* case, on the other hand, virtually no upper-air data were available upstream. Surface data alone are unable to sufficiently define the three-dimensional structure of the initial perturbation. This highlights a well-known shortcoming of the applied increment correlation function (see section 2): the horizontal and vertical structure are assumed separable (cf. Lorenc 1981), but in this case a tilting function might have been more appropriate (Jørgensen 1986).

We were not able to objectively verify these statements that explain the differences between the treatment of the two storms, but if they are correct, we may expect the impact of the scatterometer data to be enhanced in the presence of upper-air data.

From satellite measurements of atmospheric radiation spectra the vertical temperature structure of the atmosphere can be obtained. The *TIROS-N* Operational Vertical Sounder (TOVS) retrieves vertical height profiles from these measurements. Meteorological data assimilation schemes for TOVS are still further developed (Flobert et al. 1989). However, when *ERS-1* is launched, the combined impact of wind scatterometer winds and TOVS should be tested. It could be stronger than their separate effects.

7. Conclusions

We have seen that in the case study on the *QE II* storm our LAM performed very well; both the analyses and (short-term) forecasts are superior to the results obtained by other operational models. The SCAT-minus-NOSCAT analysis differences show small-scale

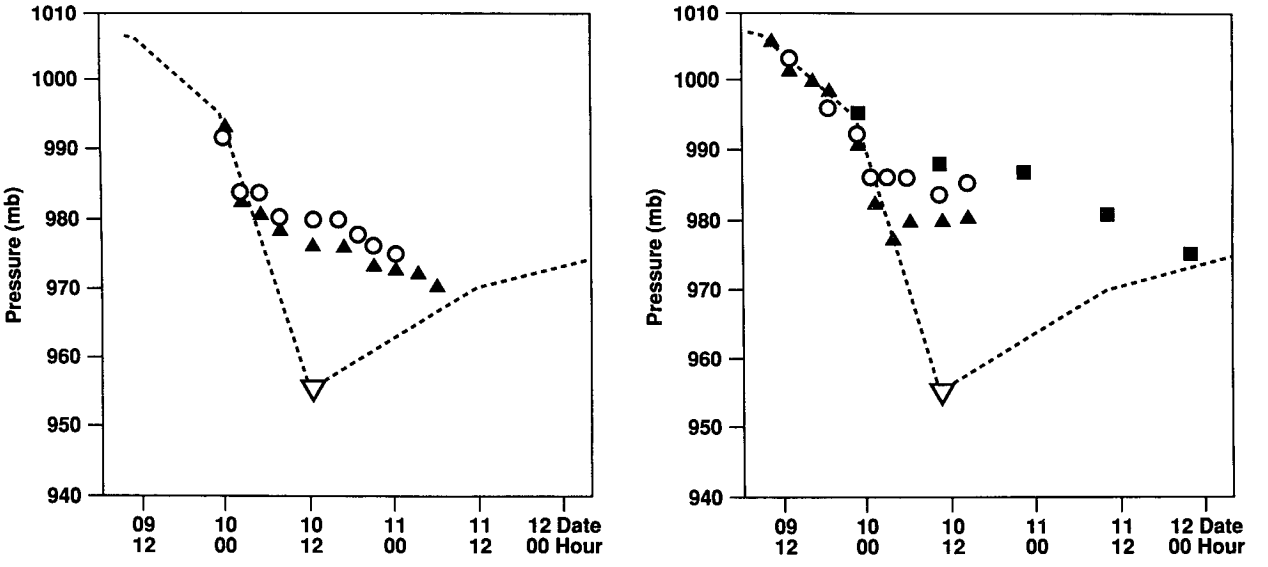

FIG. 8. Time evolution of minimum surface pressure as forecast by: □ ECMWF, ○ LAM NOSCAT, and ▲ LAM SCAT. (a) Forecast from 1200 UTC 9 September 1978. (b) Forecast from 0000 UTC 10 September 1978. The broken line is the same as in Fig. 7a.

coherent structures. These features are not damped by subsequent initialization and model integration. SCAT analyses and forecasts describe the evolution of the *QE II* storm significantly better than the NOSCAT analyses and forecasts. Therefore, we conclude that these structures contain some essential meteorological information. Even the SCAT forecast from the analysis of 0000 UTC 10 September is better, although in four analysis cycles no relevant SASS winds were assimilated. This indicates that the extra meteorological information, due to SASS observations is only slowly lost in subsequent assimilation cycles. An important reason for this may be the scarcity of conventional observations over the ocean areas. So, in the *QE II* storm case the scatterometer data is able to further improve the forecasts.

In the *Ark Royal* storm case (in an European–Atlantic area) assimilation and forecast experiments with our LAM show that the impact of the scatterometer is not significantly positive; both SCAT and NOSCAT forecasts are of poor quality. Our explanation for this relatively small impact is the lack of accurate upper-air information and the deficient manner single-level observations are treated in the analysis scheme.

We should bear in mind that we did not alter the

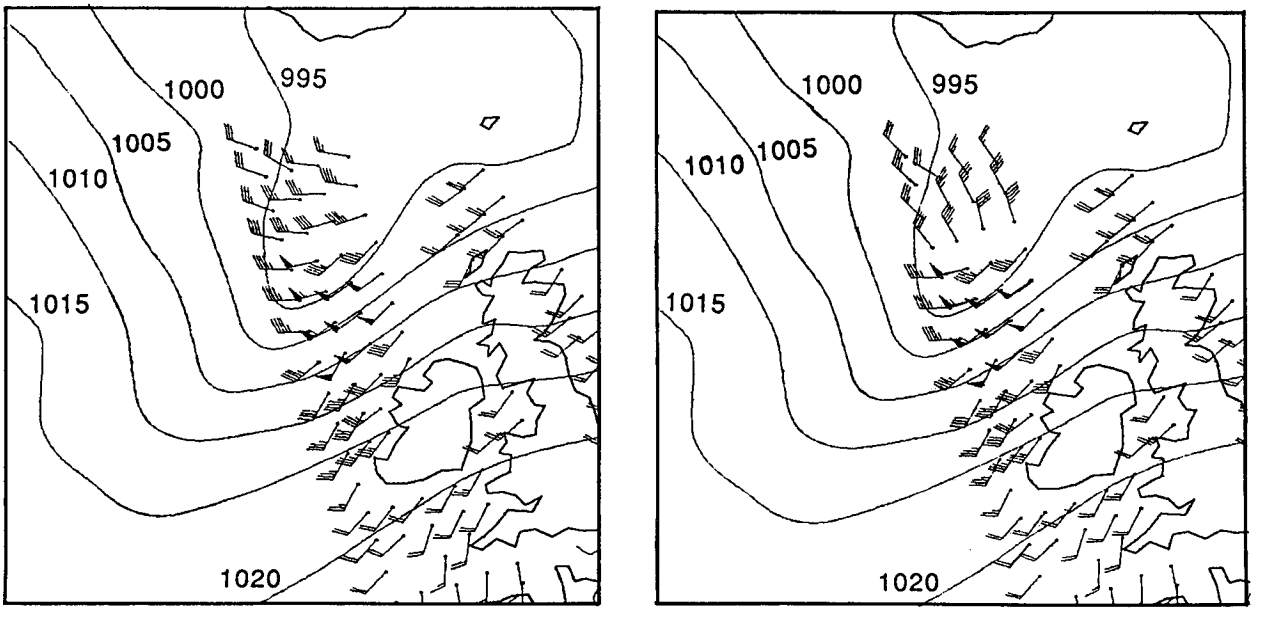

FIG. 9. Scatterometer winds in the vicinity of the developing *Ark Royal* storm: (a) Winds as dealiased by Wurtele et al. (1982); and (b) winds dealiased according to the SCAT LAM guess field, which is plotted as background.

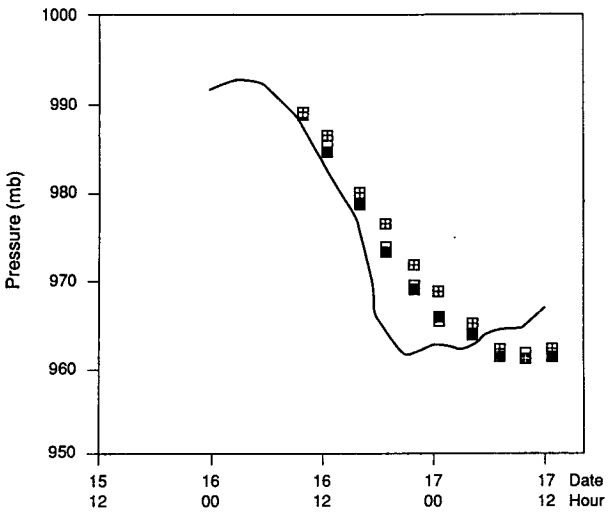

FIG. 10. Minimum pressure analyzed by the SCAT analyses (—), predicted by the NOSCAT (⊞) and SCAT (□) forecasts, and by the SCAT forecasts after changing the alias wind solutions ■.

analysis scheme to deal with this new type of spatially dense, correlated, and asynoptic measurements. Thorough research is needed to do this in an acceptable way. However, we believe that an adaptation of the assimilation methods and a well-represented upper-air structure could further enhance the impact of scatterometer wind measurements in fine-mesh NWP models. Our work indicates potential for *ERS-1* data to improve high-resolution numerical weather prediction.

Acknowledgments. We are indebted to Leo Hafkenscheid, who gave some useful comments on our work and results, and Fons Baede, who was the initiator of the project in the framework in which this work was carried out. We are grateful to Henk Tennekes for a critical review of the manuscript. Dave Anderson gave us access to the SASS data and the global meteorological fields, part of which we used for our lateral boundaries and initial conditions. The project was partly financed by The Netherlands Remote Sensing Board (BCRS).

REFERENCES

Anderson, D., A. Hollingsworth, S. Uppala and P. M. Woiceshyn, 1987: A study of the feasibility of using sea and wind information from the *ERS-1* satellite. Part I: Wind scatterometer data. European Space Agency Contract Rep. [Available from ECMWF library, Shinfield Park, Reading, Berkshire, RG2 9AX, United Kingdom.]

Anthes, R. A., Y.-H. Kuo and J. R. Gyakum, 1983: Numerical simulations of a case of explosive marine cyclogenesis. *Mon. Wea. Rev.*, **111,** 1174–1188.

Aune, R. M., and T. T. Warner, 1983: Impact of SEASAT wind data on a statistically initialized numerical model. *Sixth Conf. on Numerical Weather Prediction,* Omaha, NE, Amer. Meteor. Soc.

Baker, W. E., R. Atlas, E. Kalnay, M. Halem, P. M. Woiceshyn, S. Peteherych and D. Edelmann, 1984: Large scale analysis and forecast experiments with wind data from the *SEASAT-A* scatterometer. *J. Geophys. Res.*, **89, D3,** 4927–4936.

Brown, R. A., and G. Levy, 1986: Ocean surface pressure fields from satellite sensed winds. *Mon. Wea. Rev.*, **114,** 2197–2206.

Bijlsma, S. J., and L. M. Hafkenscheid, 1986: Initialization of a limited area model: Comparison between nonlinear normal mode and bounded derivative methods. *Mon. Wea. Rev.*, **114,** 1445–1455.

Cats, G. J., 1984: A scheme for mass and wind analysis on a limited area using multivariate three-dimensional O/I, KNMI TR-46. [Available from KNMI-Library, Postbus 201, 3730 AE, De Bilt, The Netherlands.]

Duffy, D. G., R. Atlas, T. Rosmond, E. Barker and D. Rosenberg, 1984: The impact of SEASAT scatterometer winds on the Navy's operational model. *J. Geophys. Res.*, **89, D5,** 7238–7244.

——, and ——, 1986: The impact of *SEASAT-A* scatterometer data on the numerical prediction of the *QE II* storm. *J. Geophys. Res.*, **91, 2,** 2241–2248.

European Meteorological Bulletin, 1978: Paper of the German Weather Service. Vol. 3, numbers 250–260. [Available from Deutches Wetterdienst, Zentralamt, D.6050, Offenbach am Main, Germany.]

Flobert, J. F., E. Anderson, A. Chedin, G. Kelly, J. Pailleux and N. A. Scott, 1989: Data assimilation and forecast experiments at ECMWF using the 3I retrieval scheme for satellite soundings, ECMWF Tech. Memo. 156, 45–55. [Available from ECMWF library, Shinfield Park, Reading, Berkshire, RG2 9AX, United Kingdom.]

Gyakum, J. R., 1983a: On the evolution of the *QE II* storm. Part I: Synoptic aspects. *Mon. Wea. Rev.*, **111,** 1137–1155.

——, 1983b: On the evolution of the *QE II* storm. Part II: Dynamic and thermodynamic structure. *Mon. Wea. Rev.*, **111,** 1156–1173.

Jørgenson, A. M. K., 1986: Modelling of isotropic and tilting structure functions for a statistical analysis scheme. Danish Meteorological Institute Tech. Rep. [Available from DMI library, Lyngbyvej 100, DK-2100 Copenhagen, Denmark.]

Lorenc, A. C., 1981: A global three-dimensional multivariate statistical interpolation scheme. *Mon. Wea. Rev.*, **109,** 701–721.

Louis, J. F., 1979: ECMWF forecast model documentation manual. [Available from ECMWF library, Shinfield Park, Reading, Berkshire RG2 9AX, United Kingdom.]

Pierson, W. J., 1983: Highlights of the SEASAT-SASS program: A review. *Satellite Microwave Remote Sensing.* T. D. Allan, ed. Ellis Horwood Ltd., 69–86.

Roquet, H., and A. Ratier, 1988: Towards direct variational assimilation of scatterometer backscatter measurements into numerical weather prediction models. *IGARSS '88—Remote Sensing: Moving Towards the 21st Century,* T. D. Guyenne, and J. J. Hunt, Ed., 284 pp, pwd. European Space Agency, Paris.

Stoffelen, A. C. M., G. J. Cats, L. M. Hafkenscheid and A. P. M. Baede, 1990: Impact of SASS wind data on analyses and forecasts of a fine mesh limited area model, BCRS Project Rep. TO-1.6. [Available from authors, KNMI, postbus 201, 3730 AE De Bilt, The Netherlands.]

Woiceshyn, P. M., M. G. Wurtele, D. H. Boggs, L. F. McGoldrick and S. Peteherych, 1986: The necessity for a new parameterization of an empirical model for wind–ocean scatterometry. *J. Geophys. Res.*, **91, C2,** 2273–2288.

Wurtele, M. G., P. M. Woiceshyn, S. Peteherych, M. Borowski and W. S. Appleby, 1982: Wind direction alias removal studies of *SEASAT* scatterometer derived wind fields. *J. Geophys. Res.*, **87, C5,** 3365–3377.

Yu, Y.-H., and R. D. McPherson, 1984: Global assimilation experiments with scatterometer winds from *SEASAT-A. Mon. Wea. Rev.*, **112,** 368–376.